Inorganic Chemistry

ARTICLE

pubs.acs.org/IC

Ni_5, Ni_8, and Ni_{10} Clusters with 2,6-Diacetylpyridine-dioxime as a Ligand

Albert Escuer,*[,†] Jordi Esteban,[†] and Olivier Roubeau[‡]

[†]Departament de Química Inorgànica and Institut de Nanociència i Nanotecnologia de la Universitat de Barcelona (IN2UB), Martí i Franqués 1-11, 08028 Barcelona, Spain

[‡]Instituto de Ciencia de Materiales de Aragón (ICMA), CSIC and Universidad de Zaragoza, Departamento de Física de la Materia Condensada, Pedro Cerbuna 12, 50009 Zaragoza, Spain

Supporting Information

ABSTRACT: In the present work, novel coordination possibilities for the system $dapdoH_2/Ni^{II}$ ($dapdoH_2$ = 2,6-diacetylpyridine-dioxime) have been explored. Depending on the starting reagents and solution conditions, several clusters with nuclearities ranging from Ni_5 to Ni_{10} were achieved and structurally characterized, namely, $[Ni_5(R\text{-}COO)_2(dapdo)_2(dapdoH)_2(N(CN)_2)_2(MeOH)_2]$ in which $R\text{-}COO^-$ = benzoate (**1**) or 3-chlorobenzoate (**2**), $[Ni_8(dapdo)_4(NO_3)_4(OH)_4(MeOH)_4]$ (**3**), and $[Ni_{10}(dapdo)_8(N(CN)_2)_2(MeO)(MeOH)](NO_3)$ (**4**). For the first time, pentadentate coordination for the $dapdo^{2-}$ ligand has been established. All compounds show a combination of square-planar and octahedrally coordinated nickel atoms. According to the $Ni_2(sp)Ni_3(Oh)$ (**1** and **2**), $Ni_4(sp)Ni_4(Oh)$ (**3**), and $Ni_4(sp)Ni_6(Oh)$ (**4**) environments, these systems magnetically behave as trimer, tetramer, and hexanuclear clusters, respectively. dc magnetic measurements in the 2−300 K range of temperature reveal antiferromagnetic coupling for all compounds, and the correlation of the superexchange interaction with the torsion angles involving the oximato bridges is experimentally confirmed.

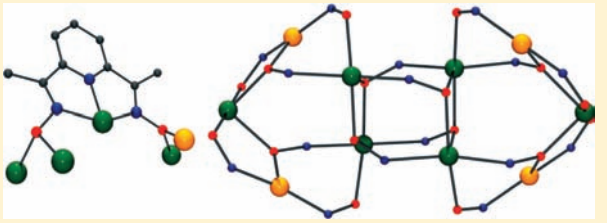

INTRODUCTION

At present, research based on the use of oximes in coordination chemistry is a growing field. 2-Pyridyl oximes, {py}C(R)-NOH, are well-known ligands in this area due to their ability to generate stable first-row transition coordination compounds with a large range of nuclearities.[1] These molecules are very versatile and able to act as bidentate ligands in their protonated state or to link up to three metallic centers in their deprotonated anionic form. In addition, the donor properties of the {py}C-(R)NOH ligands can be tuned according to the nature of the R group (H, Me, Ph, py, $-NH_2$, etc.). Self-assembly of nickel-{py}C(R)NO^- fragments have yielded a large number of medium-high nuclearity clusters, as for example, Ni_7,[2] Ni_8,[3] Ni_9,[4] Ni_{10},[5] Ni_{12}, or Ni_{14},[3,6] exhibiting, in some cases, slow relaxation of magnetization.[7]

One of the synthetic challenges in the search of high nuclearity systems is the design of ligands able to stabilize large nuclearities and/or generate new topologies in order to improve the desired properties. Regarding this matter, pyridyldioximato ligands (LH_2, with R = various) (Scheme 1) are attractive ligands for the achievement of polynuclear clusters because the three nitrogen atoms give an excellent chelate that easily coordinates one metallic center, whereas the two *ortho*-oximato groups are able to coordinate at both sides of the central cation up to four additional cations as a function of the degree of deprotonation of the ligand.

Within this family of linkers, 2,6-diacetylpyridine-dioxime ($dapdoH_2$) is the most studied among the few related ligands that have been reported to date,[1] such as 2,6-pyridinedioxime ($pdoH_2$) or pyridine-2,6-diamidoxime ($pdamoH_2$) (Scheme 1).

The most common coordination mode of these LH_2, LH^-, or L^{2-} ligands is the 1.00111 mode (Harris notation, referred to as $X.Y_1Y_2Y_3...Y_n$, where X is the overall number of metals bound by the whole ligand and each value of Y refers to the number of metal ions attached to the different donor atoms. The ordering of Y is listed by the Cahn−Ingold−Prelog priority rules, hence here O before N),[8] in which the tridentate coordination of the three nitrogen atoms yields octahedral mononuclear $[M^{II}(LH_2)_2]^{2-}$,[9] $[M^{II}(LH)_2]$,[10] or $[M^{IV}(L)_2]$[11] complexes or plays the role of terminal ligand in a number of mononuclear[12] or polynuclear[9c,13] derivatives bridged by other ligands, such as halides, pseudohalides, or carboxylates.

Larger nuclearities have been characterized, mainly in the very recent years, allowing the characterization of an increasing number of coordination modes. After the early characterization of the LH^- 2.10111 mode in the double oximato bridged Cu^{II} complex[14] with the formula $[Cu_2(dapdoH)_2](BF_4)_2$, several coordination modes have been reported for the deprotonated $dapdo^{2-}$ ligand (L^{2-} 3.11111/4.21111) or 3.20111 for LH^- in

Received: April 28, 2011
Published: August 19, 2011

Scheme 1. Reported LH_2 Pyridyldioxime Ligands

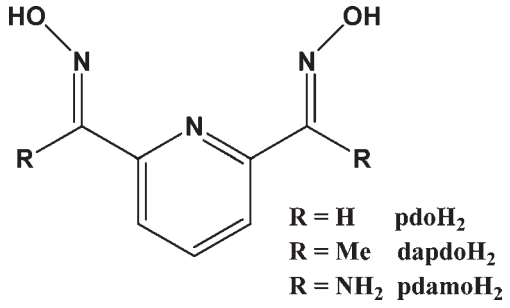

Scheme 2. Coordination Modes for $dapdoH^-$ or $dapdo^{2-}$ Ligands Found in Compounds 1−4[a]

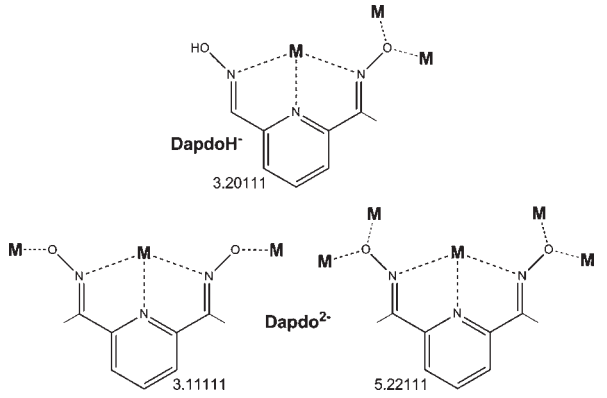

[a] The novel coordination mode 5.22111 has been observed for the first time in this work.

one mixed valence Fe_3 complex,[9d] several $Mn^{II}_2Mn^{III}_4$ and one $Mn^{II}_2Mn^{III}_6$ cluster,[15] or two heterometallic Cu^{II}/Cr^{III} and Mn^{IV}/Gd^{III} systems.[16] Our recent contribution to the knowledge of the properties of this kind of ligands comprised Cu^{II}−pdamoH_2 derivatives,[17] the first Ni^{II}−dapdoH_2 derivatives,[18] and one novel $Mn^{II}_6Mn^{III}_2$ dapdoH_2 complex[15c] in which the modes 2.10111/3.11111/3.20111 and 2.10111/3.11111/3.20111/4.21111 were found for LH^- and L^{2-}, respectively.

These previously reported complexes show how the increase of nuclearity is closely related to the deprotonation of both oximato arms, reaching the larger nuclearity reported until now (Mn_8) for the L^{2-} 4.21111 coordination mode.[15]

Following our work on pyridyldioximate ligands, we now report a series of Ni_5 (**1** and **2**), Ni_8 (**3**), and Ni_{10} (**4**) new clusters containing $dapdoH^-$ and $dapdo^{2-}$ ligands. All of them exhibit nickel centers in both octahedral or square-planar coordination environments in the same compound. For the first time, the coordination mode 5.22111 has been characterized for this kind of ligand, and larger nuclearity (M_{10}) is achieved (Scheme 2). Syntheses, structures, and magnetic behavior of **1**−**4** are described in the following sections.

EXPERIMENTAL SECTION

Syntheses. 2,6-Diacetylpyridine, $NaN(CN)_2$, and $Ni(NO_3)_2\cdot 6H_2O$ were purchased from Sigma-Aldrich Inc. and used without further purification. $Ni(BzO)_2\cdot 3H_2O$ and $Ni(3\text{-Cl-BzO})_2\cdot 3H_2O$ were synthesized by dissolving equimolar quantities (40 mmol) of benzoic acid (or 3-Cl-benzoic acid) and NaOH in 40 mL of H_2O, filtering, and mixing the final solution with a commercial source of $Ni(NO_3)_2\cdot 6H_2O$ (20 mmol) in 20 mL of water. The resulting nickel salt was obtained in good yield (>80%). dapdoH_2 was prepared following the C. W. Glynn and M. M. Turnbull method.[9a]

*[$Ni_5(RCOO)_2(dapdo)_2(dapdoH)_2(N(CN)_2)_2(MeOH)_2$] $RCOO^-$ = benzoate (**1**) or 3-Cl-benzoate (**2**).* dapdoH_2 (0.193 g, 1 mmol), $Ni(BzO)_2\cdot 3H_2O$ (0.709 g, 2 mmol) or $Ni(3\text{-Cl-BzO})_2\cdot 3H_2O$ (0.847 g, 2 mmol), and $Na(N(CN)_2)_2$ (0.178 g, 2 mmol) were dissolved in 20 mL of MeOH, and NEt_3 (0.202 g, 2 mmol) was added. The mixture was stirred for 2 h and then filtered. Crystals were obtained by layering the final solution with 10 mL of diethylether. Anal. Calcd for $C_{56}H_{54}N_{18}Ni_5O_{14}$ (**1**): C, 44.88; H, 3.77; N, 16.82%. Found: C, 44.10; H, 3.67; N, 16.65%. Anal. Calcd for $C_{56}Cl_2H_{52}N_{18}Ni_5O_{14}$ (**2**): C, 42.91; H, 3.47; N, 16.09%. Found: C, 42.31; H, 3.39; N, 15.85%. Relevant IR bands (cm^{-1}): 3432 (b), 2257 (s), 2216 (m), 2156 (s), 1594 (m), 1534 (m), 1512 (m), 1490 (m), 1377 (m), 1203 (s), 1153 (m), 1122 (m), 1087 (m), 1065 (m), 807 (w), 724 (w) for **1** and 3413 (b), 2258 (s), 2215 (m), 2156 (s), 1592 (m), 1558 (m), 1484 (m), 1407 (m), 1372 (s), 1263 (m), 1154 (m), 1086 (m), 1060 (m), 813 (w), 765 (w) for **2**.

*[$Ni_8(dapdo)_4(NO_3)_4(OH)_4(MeOH)_4$]·7MeOH (**3**·7MeOH).* Solid dapdoH_2 (0.193 g, 1 mmol) was dissolved in 20 mL of MeOH together with $Ni(NO_3)_2\cdot 6H_2O$ (0.581 g, 2 mmol) and NEt_3 (0.202 g, 2 mmol). The solution was stirred at room temperature for a couple of hours, filtered, and crystallized by layering with 10 mL of diethylether. Anal. Calcd for $C_{40}H_{56}N_{16}Ni_8O_{28}$ (**3**): C, 28.62; H, 3.36; N, 13.35%. Found: C, 27.89; H, 3.55; N, 13.00%. Relevant IR bands (cm^{-1}): 3346 (b), 1630 (w), 1591 (m), 1519 (m), 1493 (m), 1407 (s), 1384 (s), 1220 (s), 1192 (m), 1167 (w), 1131 (w), 1089 (w), 809 (m), 701 (w).

*[$Ni_{10}(dapdo)_8(N(CN)_2)_2(MeO)(MeOH)](NO_3)\cdot 3MeOH$ (**4**·3MeOH).* dapdoH_2 (0.193 g, 1 mmol), $Ni(NO_3)_2\cdot 6H_2O$ (0.581 g, 2 mmol), and $NaN(CN)_2$ (0.178 g, 2 mmol) were dissolved in 20 mL of MeOH together with NEt_3 (0.202 g, 2 mmol). The solution was stirred for 2 h and then filtered. Crystals were obtained by layering the final solution with 10 mL of diethylether. Anal. Calcd for $C_{81}H_{91}N_{31}Ni_{10}O_{24}$ (**4**·3MeOH): C, 39.39; H, 3.71; N, 17.58%. Found: C, 38.58; H, 3.52; N, 17.94%. Relevant IR bands (cm^{-1}): 3442 (b), 2267 (w), 2227 (w), 2159 (m), 1637 (m), 1592 (m), 1534 (w), 1384 (s), 1231 (w), 1205 (m), 1155 (m), 1125 (m), 1087 (m), 1086 (m), 1046 (m), 790 (w).

Physical Measurements. Magnetic susceptibility measurements were carried out on polycrystalline samples with a DSM5 Quantum Design susceptometer working in the range of 30−300 K under magnetic fields of 0.3 T and under a field of 0.03 T in the 30−2 K range to avoid saturation effects. Diamagnetic corrections were estimated from Pascal tables. Infrared spectra (4000−400 cm^{-1}) were recorded from KBr pellets on a Bruker IFS-125 FT-IR spectrophotometer.

X-ray Crystallography. Data for compounds **1** and **2** were collected on red blocks at 150 K and λ = 0.7383 Å both using a single-axis HUBER diffractometer on station BM16 of the European Synchrotron Radiation Facility, Grenoble, France. Cell refinement, data reduction, and absorption corrections were done with the HKL-2000 suite.[19] The structures were solved with SIR92,[20] and the refinement and all further calculations were carried out using SHELXL-97.[21] Data for compounds **3** and **4** were collected at 100 K on, respectively, a red plate and an orange plate both on a Bruker X8 Kappa APEX II diffractometer at the Unidade de Raios X, RIAIDT, University of Santiago de Compostela, Spain. The structures were solved by direct methods and refined on F^2 using the SHELX-TL suite.[21]

All non-hydrogens were refined anisotropically, whereas hydrogens were placed geometrically on their carrier atom and refined with a riding model where possible.

In the case of **1**, one strong electron density peak remained close to one phenyl ring and could not be included in the structural model and

dx.doi.org/10.1021/ic200895q |*Inorg. Chem.* 2011, 50, 8893–8901

Table 1. Crystal Data and Structure Refinement for Compounds 2−4

	(2)	(3)	(4)
formula	$C_{56}Cl_2H_{54}N_{18}Ni_5O_{14}$	$C_{40}H_{48}N_{16}Ni_8O_{28}\cdot 7MeOH$	$C_{78}H_{79}N_{31}Ni_{10}O_{21}\cdot 3MeOH$
fw	1567.62	1902.95	2469.95
space group	$P21/n$	$P\bar{1}$	$C2/c$
a/Å	16.980(4)	11.261(2)	15.335(3)
b/Å	11.613(3)	12.292(3)	33.125(7)
c/Å	17.846(4)	13.577(3)	21.821(4)
α/deg	90	86.48(1)	90
β/deg	118.23(3)	67.61(1)	108.18(3)
γ/deg	90	84.67(1)	90
V/Å^3	3101(2)	1729.4(6)	10531(4)
Z	2	1	4
T, K	150(2)	100(2)	100(2)
λ (Mo Kα), Å	0.73830	0.71073	0.71073
ρ_{calc}, g·cm^{-3}	1.679	1.666	1.558
μ (Mo Kα), mm^{-1}	1.832	2.433	1.826
R [$I > 2s(I)$]	0.0389	0.0584	0.0562
wR [all data]	0.1113	0.1600	0.1576
S [all data]	1.091	1.050	1.054

both R_1 and wR^2 factors remained very high at the end of the refinement, while unreasonably high EXTI and WEIGHT parameters were necessary to reach convergence. We believe the problem lies in either or both of the following: (i) strong reflections were not well treated and (ii) absorption corrections were inadequate, possibly also due to problems with strong reflections. Because compound **1** is isosutructural with compound **2**, only the structure of the latter is reported here in detail.

For compound **2**, the terminal N(6) nitrogen atom of the dicyanamide ion was highly disordered. Splitting of the atom over two positions was considered, but it did not improve the model, both half N atoms remaining highly disordered. N6 was thus refined with one sole site and displacement parameter restraints. All hydrogens were found in difference Fourier maps, and those on the oxime oxygen O(2) and methanol oxygen O(7) were refined freely with their thermal parameters 1.5 times that of their carrier O.

For compound **3**, hydrogens on the hydroxide oxygens O(3) and O(4) and on the coordinated methanol oxygens O(5) and O(8) were found in successive difference Fourier maps and refined with their thermal parameters 1.2 times that of their carrier oxygen and a soft distance restraint. Together with the four dapdo^{2-} and four-coordinated nitrate, this clearly points at a neutral main complex. The solvent area was particularly disordered. After locating one methanol molecule (O1S), the remaining electron density peaks (max. ca. five electrons) occupying a rather small void of ca. 300 Å^3 could not be modeled satisfactorily (see CIF for details). The disordered area was thus analyzed and taken into account with PLATON/SQUEEZE that recovered a total of ca. 99 electrons per cell all in one void of ca. 275 Å^3. The combination of occupied volume and electrons would account reasonably with five additional lattice methanol molecules per cell, which have been included in the formula and related structural parameters.

In the case of **4**, the terminal CN group of the dicyanamide ion was highly disordered. It was considered splitting the two atoms, but the partial atoms were still highly disordered. Therefore, C(20) and N(9) were refined with displacement parameter restraints, and their remaining high max/min ratios likely correspond to their real disorder. One of the lattice methanol molecules was only half-occupied. The coordinated methanol molecule is, in fact, half methanol and half methanoate for charge compensation. The corresponding half-occupied hydroxyl hydrogen H(9) forming a hydrogen bond with the nitrate ion was found in a difference Fourier map and refined with its thermal parameter 1.5 times that of O(9) and a distance restraint. Hydrogens on the lattice methanol molecules were omitted. At the end of the refinement, there remained areas in the structure with only weak electron density peaks that could not be modeled satisfactorily as solvent molecules. This was, therefore, analyzed and taken into account by PLATON/SQUEEZE[22] that recovered, per cell, four groups of ca. 20/70 electrons in voids of 103/267 Å^3, respectively. These figures altogether would agree with the presence of 4 methanol and 4 diethylether diffuse molecules in addition to the 12 MeOH per cell already in the structural model.

Crystallographic and experimental details for **2**−**4** are summarized in Table 1, whereas experimental details of **1** are provided in Table S1 and Figure S1 (Supporting Information). All data can be found in the supplementary crystallographic data for this paper in CIF format with CCDC numbers 817654-817657. These data can be obtained free of charge from The Cambridge Crystallographic Data Centre via www.ccdc.cam.ac.uk/data_request/cif.

Plots for publication were generated with ORTEP3 for Windows and plotted with POV-ray programs.[23]

RESULTS AND DISCUSSION

Syntheses. In our previous work,[18] we studied the reactivity of the Ni^{2+}/dapdoH$_2$/R-COO$^-$ system in a basic medium and several tri- and tetranuclear systems containing oximato and carboxylato bridges where reported, and different coordination modes for dapdoH$_2$, dapdoH$^-$, or dapdo^{2-} were characterized. The presence of labile solvent molecules in these compounds suggested the possibility to grow their nuclearity or dimensionality by means of the adequate bridging ligands. On the other hand, it was also envisaged the possibility to generate novel "empty" coordination sites by substitution of the carboxylate ligands by less coordinating anions. With this aim, we have explored the systematic reaction of nickel carboxylates with dapdoH$_2$ and additional bridging ligands, such as azide, dicyanamide, or thiocyanate. When sodium dicyanamide was present in the reaction medium, crystalline pentanuclear compounds **1** and **2** and decanuclear **4** were obtained in good yield. However,

in these compounds, the dicyanamide ligand acts as a terminal ligand and does not provide the expected linkage between polynuclear units. In contrast, reaction in the same synthetic conditions starting from nickel benzoates and sodium azide yields a mixture of dark crystals of the already reported[11] mononuclear Ni^{IV} complex $[Ni(dapdo)_2]$ containing two deprotonated $dapdo^{2-}$ ligands and red needles for which structural characterization has been unsuccessful until now. The presence of coordinated azide in its end-on coordination mode (checked by IR spectroscopy) and the ferromagnetic response of these systems suggest the probable formation of azido-containing clusters, and efforts to reach their full structural characterization are in progress.

On the other hand, the change from carboxylato anions to nitrate ones yielded the crystalline compounds **3** and **4**, which show larger nuclearity and new topologies clearly different than the carboxylato-containing complexes, suggesting a rich noncarboxylato chemistry for this ligand.

The coordination behavior of the deprotonated form $dapdo^{2-}$ bonded to Ni^{2+} atoms is remarkable. Strong spherical crystal fields, provided by the oximato groups,[24] favor the easy oxidation of the Ni^{II} cation to the d^6 low-spin Ni^{IV} oxidation state (e.g., $[Ni(dapdo)_2]$ and $[Ni(dmg)_3]^{2-}$, where dmg^{2-} stands for dimetylglioximato).[24] The square-planar environment is common for Ni^{II} atoms linked to several deprotonated oximato groups as in glioximato derivatives. However, pyridyloximato ligands give hexacoordination systematically with the only exception of the amidoxime function attached to pyridyl, pyrazyl, or pyimidinic rings, which, as in our case, give complexes in which tetra- and hexacoordination have been characterized simultaneously in the same compound.[3,6b,25] In our previous paper, we have reported how coordination of only one 3.11111 $dapdo^{2-}$ ligand it is not enough to favor the oxidation of Ni^{II} to Ni^{IV} but stabilizes the square-planar environment around the nickel centers.

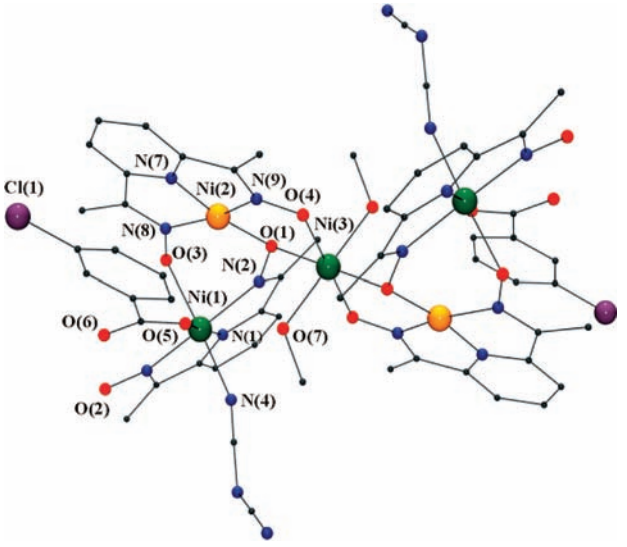

Figure 1. Labeled POV-ray plot of complex **2**. Ni atoms in an octahedral or square-planar environment are plotted in green and orange color, respectively. H atoms are omitted for clarity.

In agreement with these previous data, compounds **1**−**4** exhibit square-planar coordination for those nickel atoms linked to the three N atoms of one 3.11111 $dapdo^{2-}$ ligand. In contrast, characterization of the novel 5.22111 coordination mode shows an octahedral environment for the nickel atom coordinating the three N atoms of $dapdo^{2-}$. This feature suggests an important change in the electronic density and the reduction of the crystal field of the ligand due to the coordination of a second metallic atom to the oximato group at the limit between square-planar and octahedral environments.

Description of the Structures. *$[Ni_5(3\text{-}ClBzO)_2(dapdo)_2(dapdoH)_2(N(CN)_2)_2(MeOH)_2]$* (***2***). A labeled plot of the neutral centrosymmetric pentanuclear unit present in compound **2** is shown in Figure 1. Selected bond parameters are listed in Table 2. The pentanuclear units consist of two tetracoordinated nickel atoms Ni(2) and symmetry related Ni(2′) and three hexacoordinated nickel atoms, Ni(1), Ni(1′), and Ni(3), which are linked by the oximato groups of four ligand molecules. Each tetracoordinated cation Ni(2) is bonded to one 3.11111 $dapdo^{2-}$ molecule by its three N atoms and linked to one O-oximato atom from one neighbor $dapdoH^-$ ligand, resulting in a distorted square-planar environment. The coordination sphere of the Ni(1) cation is formed by the three N atoms of one 3.20111 $dapdoH^-$ ligand, one O-oximato atom from one neighbor $dapdo^{2-}$ ligand, one O atom from one monocoordinated benzoate group, and one N atom from one dicyanamide anion. Finally, the central Ni(3) atom is linked by four O-oximato groups (from two $dapdo^{2-}$ and two $dapdoH^-$ ligands) and by two *trans*-methanol molecules.

Ni−N bond distances are in the 1.813(2)−2.104(3) Å range, corresponding the shorter distances to the square-planar cations

Table 2. Selected Interatomic Distances (Å) and Angles (deg) for Compound 2

Ni(1)−N(1)	1.983(2)	Ni(1)−N(2)	2.070(2)
Ni(1)−N(3)	2.104(3)	Ni(1)−N(4)	2.074(2)
Ni(1)−O(3)	2.075(2)	Ni(1)−O(5)	2.035(2)
Ni(2)−N(7)	1.813(2)	Ni(2)−N(8)	1.921(2)
Ni(2)−N(9)	1.891(2)	Ni(2)−O(1)	1.881(2)
Ni(3)−O(1)	2.070 (2)	Ni(3)−O(4)	1.991(2)
Ni(3)−O(7)	2.114(2)		
Ni(1)−N(2)−O(1)	124.8(1)	Ni(1)−O(3)−N(8)	111.4(1)
Ni(2)−N(8)−O(3)	126.4(2)	Ni(1)−N(3)−O(2)	126.9(2)
Ni(2)−O(1)−N(2)	114.1(1)	Ni(2)−N(9)−O(4)	125.1(1)
Ni(3)−O(4)−N(9)	116.6(1)	Ni(3)−O(1)−N(2)	116.9(1)
Ni(2)−O(1)−Ni(3)	112.83(8)		
Ni(1)−N(2)−O(1)−Ni(2)	31.4(2)	Ni(1)−N(2)−O(1)−Ni(3)	103.3(2)
Ni(2)−N(8)−O(3)−Ni(1)	40.7(2)	Ni(2)−N(9)−O(4)−Ni(3)	6.4(2)

dx.doi.org/10.1021/ic200895q |*Inorg. Chem.* 2011, 50, 8893–8901

and being larger those provided by dapdoH$^-$ than dapdo^{2-} ligands. $N_{oxime}-Ni-N_{pyridyl}$ angles deviate from 90° due to the low bite angle of the ligand, being larger the angles generated by the dapdo^{2-} ligand (around 82°) than the angles that involve monodeprotonated dapdoH$^-$ ligands (around 77°). The torsion angle corresponding to the Ni(1)−N(1)−O(2)−Ni(3) bridge is surprisingly high, deviating only 13.3(2)° from orthogonality.

The two O atoms of the carboxylato anion participate in strong intramolecular H bonds: the coordinated O(5) atom interacts with the methanol molecule with a O(7)···O(5) distance of 2.835(3) Å, and the noncoordinated O(6) atom interacts with the protonated oximate group with a O(6)···O(2) distance of 2.635(3) Å. Aromatic rings of the dapdo^{2-} and the chlorobenzoate ligands give intercluster $\pi-\pi$ interactions with a distance between centroids of 3.495(4) Å.

[$Ni_8(dapdo)_4(NO_3)_4(OH)_4(MeOH)_4$]·3MeOH,NEt3 (***3***). Figure 2 shows a labeled plot of the neutral centrosymmetric compound **3**, while Table 3 lists the selected bond parameters. This octanuclear compound has four tetracoordinated and four hexacoordinated nickel atoms. All four tetracoordinated Ni^{II} atoms (Ni(1), Ni(3), and symmetry related) are bonded to one 3.11111 dapdo^{2-} ligand by its three N atoms and to one μ_3-OH bridging group, exhibiting a distorted square-planar geometry. Hexacoordinated Ni^{II} atoms show a NiO_6 environment and can be described as central Ni(2) and Ni(2a) and the peripheral Ni(4) and Ni(4a) groups. The central nickel atoms Ni(2) are linked by double oximato/hydroxo bridges to Ni(1a) and Ni(3) and by means of μ_3-OH groups to Ni(1), Ni(2a), and Ni(4). The coordination sphere of Ni(2) is completed with one methanol molecule. The external Ni(4) atoms are linked by double oximato/hydroxo bridges to Ni(3) and through a single oximato bridge to Ni(1). Coordination sites around Ni(4) are completed with two monodentate nitrato ligands and one methanol solvent molecule.

A set of intramolecular H bonds contribute to stabilize the molecule: O(8) from one coordinated methanol molecule interacts with O(1a) from one of the oximato groups with an (O(8)···O(1a) distance of 2.589(7) Å) and with O(3) from one of the hydroxo ligands with an (O(8)···O(3) distance of 2.941(6) Å).

One of the O atoms from one coordinated nitrato ligand interacts with the other hydroxo ligand with an O(11)···O(4) distance of 2.704(6) Å.

[$Ni_{10}(dapdo)_8(N(CN)_2)_2(MeO)(MeOH)](NO_3)$·3MeOH (***4***). A plot of the decanuclear compound **4** is shown in Figure 3. These

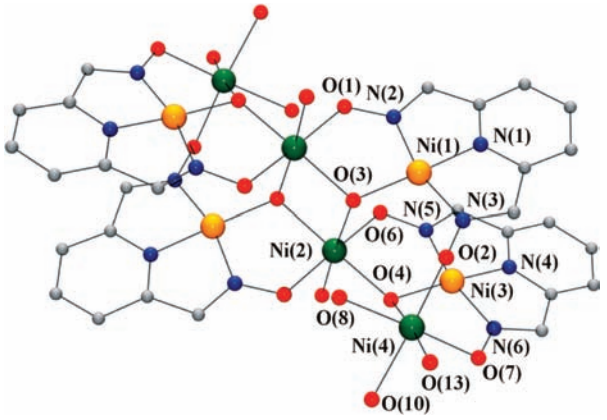

Figure 2. Labeled POV-ray plot of complex **3**. Ni atoms in an octahedral or square-planar environment are plotted in green and orange color, respectively. O(10) and O(13) correspond to oxygen atoms from coordinated nitrato ligands. H atoms are omitted for clarity.

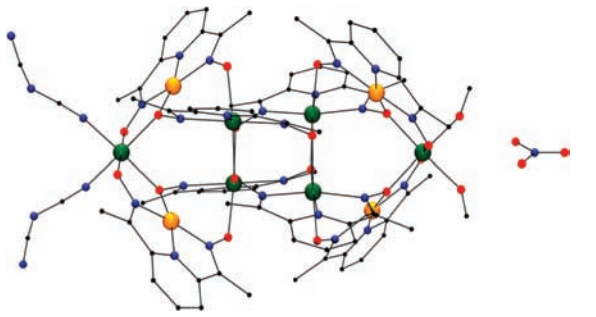

Figure 3. Plot of complex **4**. Ni atoms in an octahedral or square-planar environment are plotted in green and orange color, respectively. H atoms are omitted for clarity.

Table 3. Selected Interatomic Distances (Å) and Angles (deg) for Compound 3

Ni(1)−N(1)	1.812(5)	Ni(1)−N(2)	1.885(5)
Ni(1)−N(3)	1.902(6)	Ni(1)−O(3a)	1.853(4)
Ni(2)−O(1)	2.043(4)	Ni(2)−O(3)	2.121(4)
Ni(2)−O(3a)	2.060(4)	Ni(2)−O(4)	2.067(4)
Ni(2)−O(5)	2.076(4)	Ni(2)−O(6)	2.031(4)
Ni(3)−N(4)	1.790(5)	Ni(3)−N(5)	1.880(5)
Ni(3)−N(6)	1.874(6)	Ni(3)−O(4)	1.868(4)
Ni(4)−O(2a)	2.027(4)	Ni(4)−O(4)	2.100(4)
Ni(4)−O(7)	2.034(4)	Ni(4)−O(8)	2.075(4)
Ni(4)−O(10)	2.088(4)	Ni(4)−O(13)	2.086(5)
Ni(1a)−O(3)−Ni(2)	110.3(2)	Ni(1a)−O(3)−Ni(2a)	114.0(2)
Ni(2)−O(1)−N(2)	114.0(3)	Ni(2)−O(6)−N(5)	113.0(3)
Ni(2)−O(3)−Ni(2a)	95.5(2)	Ni(2)−O(4)−Ni(3)	109.1(2)
Ni(2)−O(4)−Ni(4)	131.3(2)	Ni(3)−O(4)−Ni(4)	105.9(2)
Ni(4a)−O(2)−N(3)	124.5(4)	Ni(4)−O(7)−N(6)	111.1(3)
Ni(4)−O(10)−N(7)	127.7(4)	Ni(4)−O(13)−N(8)	127.9(5)
Ni(1)−N(2)−O(1)−Ni(2)	10.0(6)	Ni(1)−N(3)−O(2)−Ni(4a)	76.9(5)
Ni(3)−N(5)−O(6)−Ni(2)	5.5(6)	Ni(3)−N(6)−O(7)−Ni(4)	18.9(6)

dx.doi.org/10.1021/ic200895q |*Inorg. Chem.* 2011, 50, 8893–8901

units possess a C_2 rotation axis that includes one N−O nitrato bond and the two peripheral nickel atoms. Each cluster contains six nonequivalent nickel atoms, organized as one inner $\{Ni_4(dapdo^{2-})_4\}$ pseudocubane surrounded by four nickel atoms distributed near each corner of the cube, and finally is capped by two additional peripheral nickel atoms. Six of the nickel atoms are hexacoordinated (inner cubane and peripheral ones), whereas the remainder tetracoordinated nickel ions exhibit a square-planar environment. The eight $dapdo^{2-}$ ligands are distributed in two groups: four of them link the nickel atoms of the inner cubane and adopt the unprecedented 5.22111 coordination mode, in contrast with the four $dapdo^{2-}$ ligands linked to the square-planar nickel atoms, which adopt the 3.11111 coordination mode. The two peripheral nickel atoms placed on the C_2 axis do not coordinate additional pyridyldioximato ligands.

A labeled plot of the core of the cationic decanuclear unit of **4** is depicted in Figure 4, and selected bond parameters are listed in Table 4. The octahedral coordination environment for the terminal Ni(1) atom consists of four O-oximato atoms (from two 5.22111 and two 3.11111 $dapdo^{2-}$ ligands) and two dicyanamides, giving a NiN_2O_4 environment, in contrast with Ni(6), which exhibits a NiO_6 environment from four oximato bridges (two 5.22111 and two 3.11111 $dapdo^{2-}$ ligands) and one metoxo and one methanol molecule.

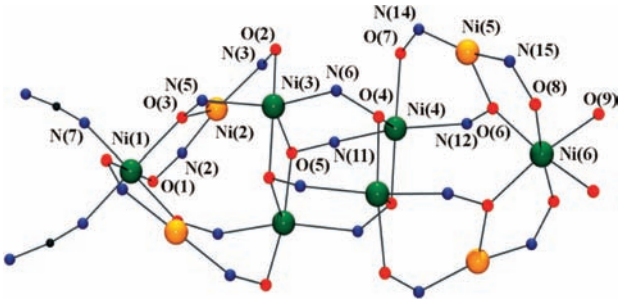

Figure 4. Labeled POV-ray plot of the core of complex **4**.

Tetracoordinated Ni(2), Ni(5), and symmetry related atoms show a square-planar environment. Each Ni^{II} atom is bonded to one 3.1111 $dapdo^{2-}$ molecule by the three N atoms and to one O-oximato group from another $dapdo^{2-}$ molecule (NiN_3O environment). Bond distances are between 1.79(1) and 1.935(7) Å, corresponding the shorter ones to the Ni−N(ring) bond. Bond angles deviate from the ideal 90° value due to the small bite of the $dapdo^{2-}$ ligand.

The hexacoordinated Ni(3), Ni(4), and symmetry related atoms form the inner $[Ni_4(NO)_4]$ pseudocubane in which each nonmetallic vertex has been substituted by one oximate bridge (Figure 5). Each oximato group provides three edges and one vertex of the pseudocube, resulting in four similar hexagonal $Ni_2(NO)_2$ faces and two conventional Ni_2O_2 square faces, with bond angles Ni(3)−O(5)−Ni(3a) and Ni(4)−O(4)−Ni(4a) of 101.0(3)° and 101.5(3)°, respectively. Ni−O−N−Ni torsion angles in the pseudocube are close to 70° in all cases. Ni(3) and Ni(4) are bridged by one single oximato bridge to Ni(1) and Ni(6), respectively, with a similar torsion angle close to 120°.

The anionic nitrate molecule interacts with the methanol/methanoate ligands coordinated to Ni(6) via a multicentric H bond in which the minimum distances of 2.65(1) and 2.814(9) Å correspond to O(9)···O(10) and O(9)···O(9a), respectively.

Magnetic Measurements and Modelization. Room-temperature $\chi_M T$ values are 3.93 and 3.95 $cm^3\,K\,mol^{-1}$, respectively,

Table 4. Selected Interatomic Distances (Å) and Angles (deg) for Compound 4

Ni(1)−O(1)	2.025(6)	Ni(1)−N(7)	2.043(9)
Ni(1)−O(3)	2.106(6)		
Ni(2)−N(1)	1.824(8)	Ni(2)−N(2)	1.893(8)
Ni(2)−N(3)	1.924(7)	Ni(2)−O(3)	1.847(6)
Ni(3)−N(4)	1.995(8)	Ni(3)−N(5)	2.107(7)
Ni(3)−N(6)	2.187(7)	Ni(3)−O(2)	2.077(6)
Ni(3)−O(5)	2.043(7)	Ni(3)−O(5a)	2.108(6)
Ni(4)−N(10)	2.005(8)	Ni(4)−N(11)	2.175(7)
Ni(4)−N(12)	2.092(7)	Ni(4)−O(4)	2.026(7)
Ni(4)−O(7)	2.064(6)	Ni(4)−O(4a)	2.125(6)
Ni(5)−N(13)	1.79(1)	Ni(5)−N(14)	1.935(7)
Ni(5)−N(15)	1.875(8)	Ni(5)−O(6)	1.843(7)
Ni(6)−O(6)	2.067(6)	Ni(6)−O(8)	1.998(8)
Ni(6)−O(9)	2.073(7)		
Ni(3)−O(5)−Ni(3a)	101.0(3)	Ni(4)−O(4)−Ni(4a)	101.5(3)
Ni(1)−O(1)−N(2)	118.9(5)	Ni(1)−O(3)−N(5)	123.7(5)
Ni(2)−O(3)−N(5)	114.2(5)	Ni(3)−O(2)−N(3)	111.7(5)
Ni(3)−O(5)−N(11)	112.0(5)	Ni(4)−O(4)−N(6)	111.5(5)
Ni(4)−O(7)−N(14)	113.9(5)	Ni(5)−O(6)−N(12)	113.1(5)
Ni(6)−O(6)−N(12)	124.3(5)	Ni(6)−O(8)−N(15)	117.9(6)
Ni(1)−O(1)−N(2)−Ni(2)	12.8(9)	Ni(1)−O(3)−N(5)−Ni(3)	119.7(5)
Ni(2)−O(3)−N(5)−Ni(3)	37.4(7)	Ni(3)−N(6)−O(4)−Ni(4)	45.0(6)
Ni(2)−N(3)−O(2)−Ni(3)	36.0(8)	Ni(4)−N(11)−O(5)−Ni(3)	45.6(7)
Ni(3)−N(6)−O(4)−Ni(4a)	69.6(6)	Ni(4)−N(11)−O(5)−Ni(3a)	69.7(7)
Ni(4)−N(12)−O(6)−Ni(5)	43.1(8)	Ni(4)−N(12)−O(6)−Ni(6)	117.0(6)
Ni(5)−N(14)−O(7)−Ni(4)	33.4(9)	Ni(5)−N(15)−O(8)−Ni(6)	16.7(9)

dx.doi.org/10.1021/ic200895q |*Inorg. Chem.* 2011, 50, 8893–8901

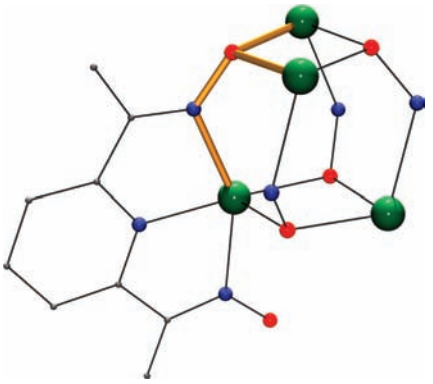

Figure 5. Pseudocube subunit of complex **4** generated by four dapdo^{2-} ligands. Each ligand provides three edges and one vertex of the pseudocube.

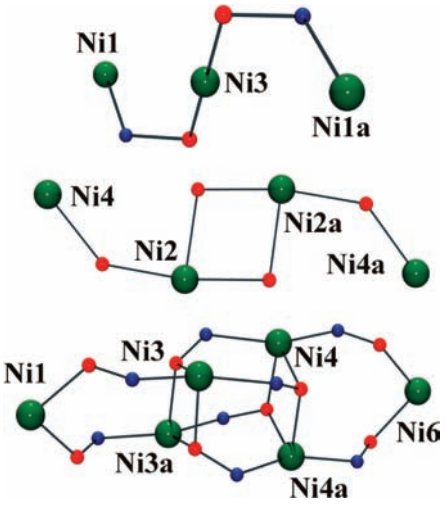

Figure 6. Core of the bridges between paramagnetic centers of compounds **1** and **2** (top), **3** (middle), and **4** (bottom). Nickel atom numbering corresponds to the subindexes of the local spin carriers S_n employed in the corresponding Hamiltonians.

for compounds **1** and **2**, 4.82 cm^3 K mol^{-1} for compound **3**, and 7.39 cm^3 K mol^{-1} for **4**, in good agreement with structural data, which reveals three, four, and six octahedral paramagnetic Ni^{II} centers, respectively. Numbering of the paramagnetic centers employed in the Hamiltonian expressions and the bridges between these atoms are plotted in Figure 6.

Compounds **1** and **2** show a $\chi_M T$ value nearly constant between 300 and 10 K, decreasing slightly at low temperature down to a minimum value of 1.98 cm^3 K mol^{-1} for **1** and 1.71 cm^3 K mol^{-1} at 1.8 K (Figure 7). The fit of the experimental data as a linear trinuclear system was calculated by means of the MAGPACK program,[26] for three local $S = 1$ spins derived from the Hamiltonian

$$H = -J(S_1 \cdot S_3 + S_3 \cdot S_{1a}) + DS_z^2$$

Best fit parameters were $J = -0.4(1)$ cm^{-1}, $g = 2.279(2)$, and $D = -3.7(2)$ for compound **1** and $J = -0.5(1)$ cm^{-1}, $g = 2.285(2)$, and $D = -3.2(2)$ for complex **2**.

The $\chi_M T$ plot for compound **3** decreases continuously on cooling and tends to zero at low temperature. χ_M increases from room temperature up to a well-defined maximum of

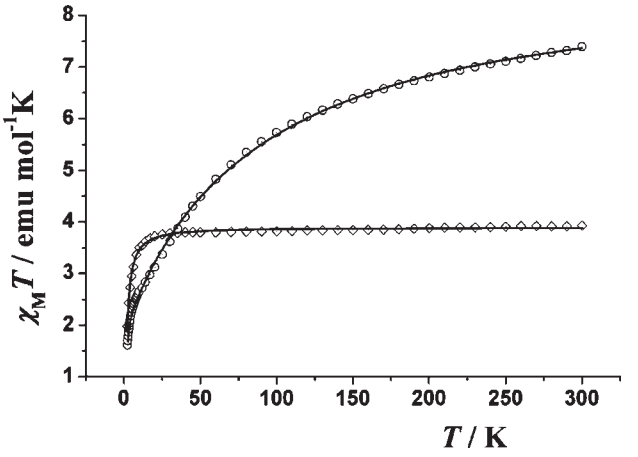

Figure 7. Plot of the $\chi_M T$ product vs T for compounds **2** (diamonds) and **4** (dot centered circles). The solid lines show the best fit of the experimental data. Compounds **1** and **2** give practically equal magnetic responses, and only the plot of **2** is shown for clarity.

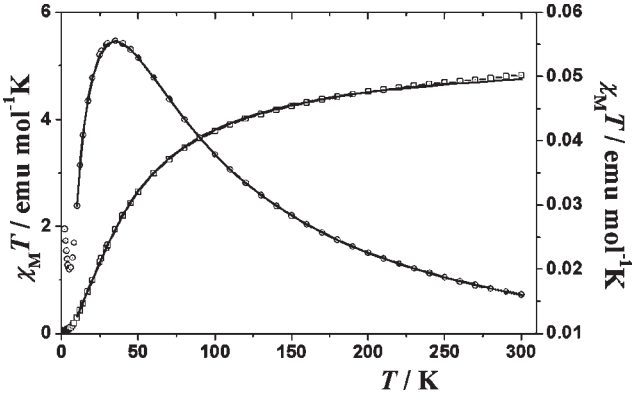

Figure 8. Plot of the $\chi_M T$ product vs T for compound **3** (squares, left axis) and χ_M vs T (dot centered circles, right axis). The solid lines show the best fit of the experimental data in the 10−300 K range of temperature.

susceptibility centered at 35 K (Figure 8). Compound **3** behaves magnetically as a tetranuclear system with two well-differentiated superexchange pathways (single or double hydroxo bridges with different Ni−O−Ni bond angles). Simulation of the experimental data was thus performed using the CLUMAG program[27] and applying the Hamiltonian

$$H = -J_1(S_2 \cdot S_4 + S_{2a} \cdot S_{4a}) - J_2(S_2 \cdot S_{2a})$$

Best fit parameters were $J_1 = -24.6$ cm^{-1}, $J_2 = -13.2$ cm^{-1}, and $g = 2.302$, with $R = 3.6 \times 10^{-5}$ ($R = (\chi_M T_{calc} - \chi_M T_{obs})^2/(\chi_M T_{obs})^2$.

The $\chi_M T$ plot for compound **4** decreases continuously on cooling from the room temperature value of 7.39 cm^3 K mol^{-1}. The plot shows a small change of slope at 13 K, reaching a value of 1.50 cm^3 K mol^{-1} at 2 K. The χ_M plot does not exhibit a maximum of susceptibility, and magnetization measurements show a quasi saturated value equivalent to four electrons under an external field of 5 T.

According to the coupling scheme of Figure 6, this system behaves as a two-J cubane capped by two additional Ni^{II} atoms linked by single oximato bridges. Bond parameters for the

dx.doi.org/10.1021/ic200895q |*Inorg. Chem.* 2011, 50, 8893–8901

oximato bridges between Ni(1) with Ni(3)/Ni(3a) and Ni(6) with Ni(4)/Ni(4a) are very similar, and thus, to minimize the number of coupling constants in the fitting process, we have assumed greater symmetry than that experimentally found in the structure. Simulation was performed by means of the CLUMAG program[27] applying the three-J Hamiltonian

$$H = -J_1(S_1 \cdot S_3 + S_1 \cdot S_{3a} + S_6 \cdot S_4 + S_6 \cdot S_{4a}) - J_2(S_3 \cdot S_{3a} + S_4 \cdot S_{4a}) - J_3(S_3 \cdot S_4 + S_3 \cdot S_{4a} + S_{3a} \cdot S_4 + S_{3a} \cdot S_{4a})$$

Best fit parameters were $J_1 = -4.8$ cm^{-1}, $J_2 = -26.2$ cm^{-1}, $J_3 = -24.6$ cm^{-1}, and $g = 2.390$ with $R = 2.1 \times 10^{-5}$.

Correlations for the coupling in Cu^{II} or Mn^{III} oximato bridged systems have been well-established in the last recent years and taking into account the orbitals of the Ni^{II} cation involved in the superexchange interaction has been widely assumed a response closer to Cu^{II} (decrease of the antiferromagnetic interaction with the increase of the M−O−N−M torsion angle)[28] than Mn^{III} (strong dependence of J with the torsion with even reversal of the sign of the coupling constants for torsion angles around 30° in triangular compounds).[29] Very recently, on the basis of experimental correlations on the Ni−O−N−Ni pathway, an intermediate response between Cu^{II} and Mn^{III} has been proposed,[30] suggesting a decrease of the antiferromagnetic interaction for increasing torsions up to around 75−80°, at which point the switch to ferromagnetic interaction may be possible. The quasi negligible values of J found for compounds **1** and **2** provide a nice example of the magnetic response of the system Ni−O−N−Ni with large torsion angles close to orthogonality. As was suggested, this superexchange pathway experimentally reveals to transmit a quasi negligible interaction in contrast with the well-established medium-strong antiferromagnetic coupling widely reported for planar or weakly distorted bridges.[1]

Compound **4** contains two kinds of oximato bridges with different torsion angles: large Ni−O−N−Ni torsions are found for the bridges between the peripheral atoms and the central cubane unit (117.0° and 119.7°) and lower torsions (around 45° and 69°) inside the cubane. In agreement with the above general trends, the found J values show weak antiferromagnetic coupling for the bridges mediated by large torsion angles (−4.8 cm^{-1}) and medium interactions with mean J values around −25 cm^{-1} for the less-distorted bridges.

The remainder of interactions in compound **4** and those found in **3** follow the well-established correlations for Ni−O−Ni bond angles with increasing antiferromagnetic interaction for larger bond angles.[26]

CONCLUSIONS

In the present work, we have reported a new series of Ni^{II} clusters obtained using the dioximato ligand dapdoH_2 in carboxylato and noncarboxylato chemistry. The most relevant features have been the characterization of the larger cluster reported until now containing pyridyldioximato ligands and the new 5.22111 coordination mode characterized for the deprotonated form dapdo^{2-}, which spreads the picture of the coordination possibilities of this kind of ligand. It becomes also relevant that, in contrast with the well-known 3.11111 coordination mode that systematically generates a square-planar coordination around the Ni^{II} cations or even favors the easy oxidation to Ni^{IV}, the new 5.22111 mode stabilizes octahedral environments. Analysis of the calculated coupling constants provides experimental examples of the predicted response of the Ni−O−N−Ni pathway with large torsion angles.

ASSOCIATED CONTENT

Supporting Information. Crystallographic data files (CIF format) for complexes **2**−**4**, crystal data (Table S1), and plot of compound **1** (Figure S1). This material is available free of charge via the Internet at http://pubs.acs.org.

AUTHOR INFORMATION

Corresponding Author
*E-mail: albert.escuer@ub.edu.

ACKNOWLEDGMENT

This work was supported by the CICYT projects CTQ2009-07264. A.E. acknowledges the support of the ICREA-Academia Research Award. The authors are grateful to Dr. G. Aromí, Universitat de Barcelona, and to the Spanish MCI for facilitating access to BM16 at ESRF (EXP16-01-739).

REFERENCES

(1) Milios, C. J.; Stamatatos, T. C.; Perlepes, S. P. *Polyhedron* **2006**, *25*, 134.

(2) Stamatatos, T. C.; Diamantopoulou, E.; Raptopoulou, C. P.; Psycharis, V.; Escuer, A.; Perlepes, S. P. *Inorg. Chem.* **2007**, *46*, 2350.

(3) Ji, C.-M.; Yang, H.-J.; Zhao, C.-C.; Tangoulis, V.; Cui, A.-L.; Kou, H.-Z. *Cryst. Growth Des.* **2009**, *9*, 4607.

(4) (a) Pajunen, A.; Mutikainen, I.; Saarinen, H.; Orama, M. *Z. Kristallogr. - New Cryst. Struct.* **1999**, *214*, 217. (b) Khanra, S.; Weyhermuller, T.; Rentschler, E.; Chaudhuri, P. *Inorg. Chem.* **2005**, *44*, 8176. (c) Stamatatos, T. C.; Diamantopoulou, E.; Tasiopoulos, A.; Psycharis, V.; Vicente, R.; Raptopoulou, C. P.; Nastopoulos, V.; Escuer, A.; Perlepes, S. P. *Inorg. Chim. Acta* **2006**, *359*, 4149. (d) Stamatatos, T. C.; Papatriantafyllopoulou, C.; Katsoulakou, E.; Raptopoulou, C. P.; Perlepes, S. P. *Polyhedron* **2007**, *26*, 1830.

(5) Psomas, G.; Dendrinou-Samara, C.; Alexiou, M.; Tsohos, A.; Raptopoulou, C. P.; Terzis, A.; Kessissoglou, D. P. *Inorg. Chem.* **1998**, *37*, 6556.

(6) (a) Stamatatos, T. C.; Abboud, K. A.; Perlepes, S. P.; Christou, G. *Dalton Trans.* **2007**, 3861. (b) Papatriantafyllopoulou, C.; Jones, L. F.; Nguyen, T. D.; Matamoros-Salvador, N.; Cunha-Silva, L.; Paz, F. A. A.; Rocha, J.; Evangelisti, M.; Brechin, E. K.; Perlepes, S. P. *Dalton Trans.* **2008**, 3153. (c) Stamatatos, T. C.; Escuer, A.; Abboud, K. A.; Raptopoulou, C. P.; Perlepes, S. P.; Christou, G. *Inorg. Chem.* **2008**, *47*, 11825.

(7) Papatriantafyllopoulou, C.; Stamatatos, T. C.; Wernsdorfer, W.; Teat, S. J.; Tasiopoulos, A.; Escuer, A.; Perlepes, S. P. *Inorg. Chem.* **2010**, *49*, 10486.

(8) Coxall, R. A.; Harris, S. G.; Henderson, D. K.; Parsons, S.; Tasker, P. A.; Winpenny, R. E. P. *J. Chem. Soc., Dalton Trans.* **2000**, 2349.

(9) (a) Glynn, C. W.; Turnbull, M. M. *Transition Met. Chem.* **2002**, *27*, 822. (b) Halcrow, M. A.; Kilner, C. A.; Wolowska, J.; McInnes, E. J. L.; Bridgeman, A. J. *New J. Chem.* **2004**, *28*, 228. (c) Bovenzi, B. A.; Pearse, G. A., Jr. *J. Chem. Soc., Dalton Trans.* **1997**, 2793. (d) Vasilevsky, I. V.; Stenkamp, R. E.; Lingafelter, E. C.; Rose, N. J. *J. Coord. Chem.* **1988**, *19*, 171.

(10) Salonen, M.; Saarinen, H.; Mutikainen, I. *J. Coord. Chem.* **2008**, *61*, 1462.

(11) (a) Sproul, G.; Stucky, G. D. *Inorg. Chem.* **1973**, *12*, 2898. (b) Namli, H.; Azaz, A. D.; Karabulut, S.; ÇElen, S.; Kurtaran, R.; Kazak, C. *Transition Met. Chem.* **2007**, *32*, 266.

(12) (a) Nicholson, G. A.; Petersen, J. L.; McCormick, B. J. *Inorg. Chem.* **1982**, *21*, 3274. (b) Vasilevsky, I. V.; Stenkamp, R. E.; Lingafelter, E. C.; Schomaker, V.; Willett, R. D.; Rose, N. J. *Inorg. Chem.* **1989**, *28*, 2619. (c) Abboud, K. A.; Palenik, R. C.; Palenik, G. J. *Acta Crystallogr., Sect. C* **1994**, *C50*, 525. (d) Abram, S.; Maichle-Mössmer, C.; Abram, U. *Polyhedron* **1997**, *16*, 2183. (f) Abram, S.; Maichle-Mössmer, C.; Abram, U. *Polyhedron* **1997**, *16*, 2291. (g) Singh, S. K.; Sharma, S.; Dwivedi, S. D.; Zou, R.-Q.; Xu, Q.; Pandey, D. S. *Inorg. Chem.* **2008**, *47*, 11942.

(13) (a) Unni Nair, B. C.; Sheats, J. E.; Ponteciello, R.; Van Engen, D.; Petrouleas, V.; Dismukes, G. C. *Inorg. Chem.* **1989**, *28*, 1582. (b) Marsh, R. E. *Inorg. Chem.* **1990**, *29*, 572. (c) Escuer, A.; Cordero, B.; Solans, X.; Font-Bardia, M.; Calvet, T. *Eur. J. Inorg. Chem.* **2008**, 5082.

(14) Nicholson, G. A.; Petersen, J. L.; McCormick, B. J. *Inorg. Chem.* **1980**, *19*, 195.

(15) (a) Stamatatos, T. C.; Luisi, B. S.; Moulton, B.; Christou, G. *Inorg. Chem.* **2008**, *47*, 1134. (b) Khanra, S.; Weyhermüller, T.; Chaudhuri, P. *Dalton Trans.* **2008**, 4885. (c) Escuer, A.; Cordero, B.; Font-Bardia, M.; Calvet, T.; Roubeau, O.; Teat, S. J.; Fedi, S.; Fabrizi di Biani, F. *Dalton Trans.* **2010**, *39*, 4817.

(16) (a) Khanra, S.; Weyhermüller, T.; Chaudhuri, P. *Dalton Trans.* **2007**, 4675. (b) Lampropoulos, C.; Stamatatos, T. C.; Abboud, K. A.; Christou, G. *Inorg. Chem.* **2009**, *48*, 429.

(17) Escuer, A.; Vlahopoulou, G.; Perlepes, S. P.; Font-Bardia, M.; Calvet, T. *Dalton Trans.* **2011**, *40*, 225.

(18) Escuer, A.; Esteban, J.; Aliaga-Alcalde, N.; Font-Bardia, M.; Calvet, T.; Roubeau, O.; Teat, S. J. *Inorg. Chem.* **2010**, *39*, 2259.

(19) Otwinowski, Z.; Minor, W. *Methods in Enzymology*; Carter, C. W., Jr., Sweet, R. M., Eds.; Academic Press: New York, 1997; Vol. 276: Macromolecular Crystallography, part A, pp 307−326.

(20) Altomare, A.; Burla, M. C.; Camalli, M.; Cascarano, G. L.; Giacovazzo, C.; Guagliardi, A.; Polidori, G. *J. Appl. Crystallogr.* **1994**, *27*, 475.

(21) Sheldrick, G. M. *Acta Crystallogr.* **2008**, *A64*, 112.

(22) Spek, A. L. *J. Appl. Crystallogr.* **2003**, *36*, 7.

(23) Ortep-3 for Windows: Farrugia, L. J. *J. Appl. Crystallogr.* **1997**, *30*, 565.

(24) Baucom, E. I.; Drago, R. S. *J. Am. Chem. Soc.* **1971**, *93*, 6469.

(25) (a) Kou, H.-Z.; An, G.-Y.; Ji, C.-M.; Wang, B.-W.; Cui, A.-L. *Dalton Trans.* **2010**, *39*, 9604. (b) Gole, B.; Chakrabarty, R.; Mukherjee, S.; Song, Y.; Mukherjee, P. S. *Dalton Trans.* **2010**, *39*, 9766. (c) An, G.-Y.; Ji, C.-M.; Cui, A.-L.; Kou, H.-Z. *Inorg. Chem.* **2011**, *50*, 1079.

(26) Borras-Almenar, J. J.; Clemente-Juan, J. M.; Coronado, E.; Tsukerblat, B. S. *J. Comput. Chem.* **2001**, *22*, 985.

(27) Gatteschi, D.; Pardi, L. *Gazz. Chim. Ital.* **1993**, *123*, 231.

(28) (a) Escuer, A.; Vlahopoulou, G.; Perlepes, S. P.; Font-Bardia, M.; Calvet, T. *Dalton Trans.* **2011**, *40*, 225. (b) Ruiz, R.; Lloret, F.; Julve, M.; Munoz, M. C.; Bois, C. *Inorg. Chim. Acta* **1994**, *219*, 179. (c) Colacio, E.; Dominguez-Vera, J. M.; Escuer, A.; Klinga, M.; Kivekas, R.; Romerosa, A. *J. Chem. Soc., Dalton Trans.* **1995**, 343. (d) Dominguez-Vera, J. M.; Colacio, E.; Escuer, A.; Klinga, M.; Kivekäs, R.; Romerosa, A. *Polyhedron* **1997**, *16*, 281.

(29) (a) Milios, C. J.; Inglis, R.; Vinslava, A.; Bagai, R.; Wernsdorfer, W.; Parsons, S.; Perlepes, S. P.; Christou, G.; Brechin, E. K. *J. Am. Chem. Soc.* **2007**, *129*, 12505. (b) Inglis, R.; Jones, L. F.; Milios, C. J.; Datta, S.; Collins, A.; Parsons, S.; Wernsdorfer, W.; Hill, S.; Perlepes, S. P.; Piligkos, S.; Brechin, E. K. *Dalton Trans.* **2009**, 3403.

(30) Palacios, M. A.; Mota, A. J.; Perea-Buceta, J. E.; White, F. J.; Brechin, E. K.; Colacio, E. *Inorg. Chem.* **2010**, *49*, 10156.